THE AMERICAN SOCIETY OF MECHANICAL ENGINEERS
345 E. 47th St., New York, N.Y. 10017

94-GT-453

MEASUREMENTS OF THE TIP CLEARANCE FLOW FOR A HIGH REYNOLDS NUMBER AXIAL-FLOW ROTOR: PART 1 – FLOW VISUALIZATION

W. C. Zierke, K. J. Farrell, and W. A. Straka
Applied Research Laboratory
Pennsylvania State University
State College, Pennsylvania

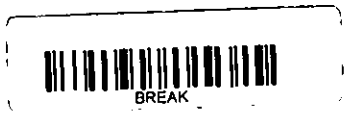

ABSTRACT

A high Reynolds number pump (HIREP) facility has been used to acquire flow measurements in the rotor blade tip clearance region--with blade chord Reynolds numbers of 3,900,000 and 5,500,000. The initial experiment involved rotor blades with varying tip clearances, while a second experiment involved a more detailed investigation of a rotor blade row with a single tip clearance. This paper focuses on flow visualization, employing techniques unique for use in water. The flow visualization on the blade surface and within the flow field indicate that the combination of centripetal acceleration and separation near the trailing edge of the rotor blade suction surface results in the formation of a trailing-edge separation vortex--a vortex which migrates radially upwards along the trailing edge and then turns in the circumferential direction near the casing, moving in the opposite direction of blade rotation. Flow visualization also helps in establishing the trajectory of the tip leakage vortex core. The trailing-edge separation vortex, which lies closer to the endwall than the tip leakage vortex, seems to have an influence on this trajectory. Finally, the periodic interaction of the rotor blades with wakes from the upstream inlet guide vanes--as well as freestream turbulence and vortex structure instabilities--affects the unsteadiness of the vortex.

NOMENCLATURE

A	amplitude of oscillation
c	blade chord
c_{tip}	blade chord at rotor tip
F_r	radial blade force
h	rotor tip clearance
K_p	pressure coefficient $= \dfrac{p - p_{ref}}{\frac{1}{2}\rho U_{tip}^2}$
p	static pressure
p_{ref}	inlet reference static pressure
r	radius (relative to tunnel axis)
r_c	vortex core radius
R_c	radius of curvature of the meridional projection of the streamlines
$Re_{c_{tip}}$	blade tip chord Reynolds number $= \dfrac{W_1 c_{tip}}{\nu}$
t_{max}	maximum blade thickness
U_{tip}	rotor blade tip speed
V	velocity (relative to tunnel coordinate system)
V_{ref}	inlet reference axial velocity
W	relative velocity
x_c	distance along the blade chord
y_c	distance normal to the camber line
γ	stagger angle
$(\Delta K_p)_{mean}$	difference in K_p across the blade at some mean radius (a radius outside the endwall region)
κ	blade metal angle
ν	kinematic viscosity
ρ	fluid density
ϕ	flow coefficient $= \dfrac{V_{ref}}{U_{tip}}$

Subscripts

m	meridional direction

Presented at the International Gas Turbine and Aeroengine Congress and Exposition
The Hague, Netherlands — June 13–16, 1994

z	axial direction
θ	tangential direction
1	blade row inlet
2	blade row exit

INTRODUCTION

Recent design trends toward high pressure ratios and low aspect ratio blading in aero-engines have re-emphasized the importance of minimizing tip clearance flow effects which degrade efficiency and stability. Research has continued over seven decades since Betz [1925] first examined tip loss in Kaplan turbines. However, it has been aerodynamic experimenters who have made steady progress in the understanding of tip clearance flows since the early flow visualization experiments of Meldahl [1941]--more so than their hydrodynamic counterparts. Studies of tip clearance effects in both compressors and turbines have evolved from single stationary blades and endwalls with a clearance to include cascades of blades, moving endwalls, and, most recently, actual rotating rigs. Both careful experimentation and three-dimensional Navier-Stokes solutions have revealed important tip clearance flow features and, yet, questions remain. Recent research has focused on mitigating leakage effects through blade tip and casing treatments. A complete commentary of the research is obviously not possible here; rather a concise description of the physical mechanisms affecting the tip leakage flow is presented. Reeder [1969], Peacock [1981], and Yaras and Sjolander [1988] have all performed reviews of tip leakage flow.

The relative motion of a turbomachinery blade and the casing at the rotor/casing endwall or the stator/hub endwall requires a finite clearance to avoid rubbing. The resulting tip clearance flow and alteration of the throughflow are driven by several mechanisms. First, the pressure difference across the blade tip forces flow through the clearance. Second, the relative motion of the blade tip and the endwall in a compressor or pump augments this inviscid leakage flow, while in a turbine, the relative motion diminishes it. Third, the endwall and blade boundary layers supply vorticity to the scraping and leakage vortices. Finally, the clearance itself determines the leakage resistance by controlling the blade tip position in the endwall boundary layer, which alters flow incidence and the wall shearing effect. While single blade and cascade experiments have revealed important results, a large experimental rig is essential to include all of these interacting mechanisms and, then, allow the opportunity to quantify them with extensive measurements upstream, downstream, in the rotor blade passages, and within the clearance. To this end, the high Reynolds number pump (HIREP) facility used in the present investigation is particularly suitable.

Axial-flow pumps and compressors are subject to many of the same design considerations in regard to tip clearance flows. However, in pumps, which are liquid handling machines, the complex flow in the tip region may lead to several types of cavitation, in addition to energy losses. In compressors, where the design is obviously not constrained by the possibility of cavitation, the intersection of the rotor pressure surface and the tip surface is purposely made sharp to promote separation and minimize the leakage mass flow rate. Pump designers, however, must assure the smooth passage of the leakage flow through the clearance to avoid flow separation and the possibility of cavitation in the gap, at the likely expense of the energy losses caused by the larger leakage mass flow rate. Designers of both types of turbomachines face the challenge of minimizing the losses associated with the vortical flows in the tip region--with the further consequence of vortex cavitation in the pump case--primarily by the leakage flow, or by the blade tip turning and stretching of the endwall boundary layer vorticity. While the study of cavitation in the tip region is certainly important, it is not the focus here. However, under similar water quality conditions, cavitation can be used as an important flow visualization tool for the structure, location, and relative strength of vortices--information which is paramount in the understanding of tip leakage flow phenomena. Moreover, the large physical size, reduced power consumption, and robustness of pump blading allow more detailed measurements and flow visualization than can be achieved in a compressor rig of comparable size and Reynolds number.

In this paper, we briefly describe the experimental facility. Then, we will present and discuss the experimental results obtained primarily from flow visualization. In the second and companion paper (Zierke, Farrell, and Straka [1994]), we will present and discuss results from detailed flow measurements.

EXPERIMENTAL FACILITY

These experiments were performed in the Garfield Thomas Water Tunnel at ARL Penn State. The tunnel has a 1.22-meter diameter, 4.27-meter long test section which supports water velocities up to 18.29 m/sec and static pressures ranging from 20 to 414 kPa. Cavitation experiments employ a water-conditioning, or bypass, system to de-gas the water. Tunnel turbulence is controlled using a honeycomb placed within the plenum, 2.82 meters upstream of the nine-to-one contraction nozzle, giving a measured axial component of the freestream turbulence intensity level to be 0.107% ± 0.006% with 95% confidence. Lauchle, Billet, and Deutsch [1989] give a detailed description of the tunnel, as well as some of the basic experimental procedures.

Figure 1 shows a schematic of the HIREP facility. HIREP consists of a 1.07-meter diameter pump stage driven by a 1.22-meter diameter downstream turbine. The hub has a constant diameter of 0.53 meters. As shown in Figure 1, the two units rotate together on a common shaft in the test section of the water tunnel--such that the main drive impeller of the tunnel overcomes the energy losses within HIREP. The pump includes a row of 13 inlet guide vanes, a row of 7 rotating blades, and three downstream support struts. The turbine includes a row of variable pitch control vanes, a row of rotating blades, and a downstream cruciform support strut. Farrell, McBride, and Billet [1987] give a more detailed explanation of the HIREP facility.

The first HIREP experiment was designed explicitly to investigate the tip leakage vortices--and the subsequent vortex cavitation--that result from varying the clearance, h, between the pump rotor blades and the casing formed by the tunnel liner. The 7 rotor blades included 5 blades with different tip clearances. The rotor blades are designed with a mild blade circumferential lean or skew (skewed in the opposite direction of blade rotation). All of the blades include fillets where the blades meet the endwalls and each rotor tip section includes a rounded pressure side corner,

with a radius of curvature of approximately 25% of the local blade thickness. Gearhart [1966] found that this rounded corner prevented local separation of the flow through the tip clearance and, thus, improved the gap cavitation performance. Table 1 presents some of the pertinent geometry and flow parameters for this HIREP design.

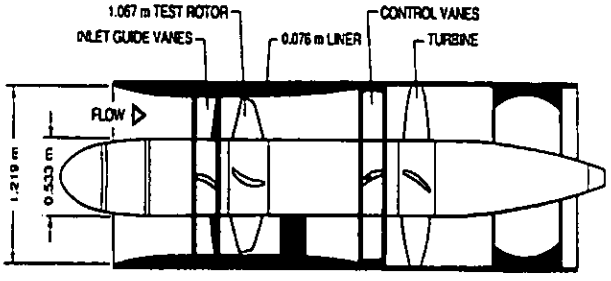

FIGURE 1. HIGH REYNOLDS NUMBER PUMP FACILITY.

The second HIREP experiment focussed on acquiring a larger quantity of data from the entire flow field of the pump, in order to establish a detailed database for use in testing numerical prediction methods. This experiment involved more lightly-loaded blades than the first experiment and, again, Table 1 gives some of the important geometry and flow parameters for this design. These rotor blades differed from the initial blade designs in that they had substantially more blade lean. However, these blades also had a rounded pressure side corner at the tip.

EXPERIMENTAL TECHNIQUE

Both the first and second experiments employed many of the same experimental techniques. For surface flow visualization, we used an oil-paint method to obtain patterns of skin-friction lines. In order to apply this type of surface flow visualization technique to rotating blades, one must be assured that the centrifugal force does not affect the oil-paint in a different manner than it affects the actual fluid. For our HIREP experiments, we combined gear oil with paint, which itself is a combination of linseed oil and pigment. With both the gear oil and linseed oil having a specific gravity near 0.94 (compared to 1.0 for water), the final oil-paint has a specific gravity close to that of water, making the added effect of centrifugal force almost negligible. Therefore, following the work of Arakawa and Tagori [1980], this type of surface flow visualization becomes applicable to blades rotating through water--as opposed to blades rotating through air. Within the flow field, the variable pressure system within the water tunnel provides a means for viewing cavitation, a technique that provides valuable flow visualization results. Since the core of the rotor tip leakage vortex has a relatively low static pressure, cavitation visualization allows one to visualize the location and extent of this important feature of the flow field. Farrell [1989] gives the details for performing this cavitation visualization.

A few experimental techniques were unique to the initial HIREP experiment--with only one being of interest to the flow visualization results. We implemented a dynamic gap measuring system to show that the low angular speed of the rotor did not change the rotor tip clearance from its static value. With this point proven, we did not implement the system in the second experiment.

TABLE 1. GEOMETRY AND FLOW PARAMETERS FOR HIREP.

Parameter	First HIREP Experiment		Second HIREP Experiment	
	Inlet Guide Vanes	Rotor Blades	Inlet Guide Vanes	Rotor Blades
Blade Number	13	7	13	7
Chord, c	0.16 m (hub) 0.20 m (tip)	0.34 m (hub) 0.21 m (tip)	0.18 m	0.29 m (hub) 0.27 m (tip)
Maximum Blade Thickness, r_{max}/c	12.0% (hub) 10.0% (tip)	15.0% (hub) 9.8% (tip)	11.6%	17.6% (hub) 10.0% (tip)
Solidity	1.25 (hub) 0.79 (tip)	1.41 (hub) 0.43 (tip)	1.36 (hub) 0.68 (tip)	1.19 (hub) 0.56 (tip)
Hub Radius	0.27 m	0.27 m	0.27 m	0.27 m
Tip Radius (nominal)	0.53 m	0.53 m	0.53 m	0.53 m
Rotor Tip Clearance, h/c_{tip}	-	1.07% 3.00% 3.54% 5.82% 5.89%	-	1.24%
Diffusion Factor	-	0.37 (hub) 0.12 (tip)	-	0.28 (hub) 0.12 (tip)
Reference Velocity, V_{ref}	11.0 m/sec		10.7 m/sec	
Rotor Rotational Speed	270 rpm		260 rpm	
Rotor Tip Velocity, U_{tip}	15.1 m/sec		14.5 m/sec	
Flow Coefficient, $\Phi = V_{ref}/U_{tip}$	0.73		0.74	
Blade Chord Reynolds Number, $Re_{c_{tip}} = W_1 c_{tip}/\nu$	3,900,000		5,500,000	

For the second HIREP experiment, within one rotor blade passage, both the pressure and suction surfaces included 40 static-pressure taps, each connected via tubing to a solid-state piezoresistive pressure transducer located near the centerline of the rotor hub. Relevant to this tip clearance flow study, the pressure taps provide measurements of the blade static-pressure distribution at 90% span, with 8 taps positioned on both the pressure and suction surface. Zierke, Straka, and Taylor [1993] showed how to correct the measured blade static pressures for the effect of rotation. A second additional experimental technique involved the visualization of the rotor tip leakage vortex in a plane normal to the axial-flow direction using a laser light sheet technique downstream of the rotor blades. In order to view the laser light sheet in the vicinity of the rotor tip clearance region, we designed a special periscope and installed it downstream of the rotor blades through the tunnel endwall liner. Using both 10 micron microballoons (with a specific gravity of 1.1) and cavitation bubbles for illumination, this flow visualization technique proved useful for locating the rotor tip leakage vortex relative to the casing endwall. Again, Zierke, Straka, and Taylor [1993] give further details of the experimental techniques used during the second HIREP experiment.

EXPERIMENTAL RESULTS

Using these techniques, we performed both experiments within HIREP in order to investigate the tip clearance flow. Since the second experiment involved a larger quantity of detailed data, we shall focus on the results from this experiment. However, results from the first experiment will also be given--especially where they give insight into the effect of a varying tip clearance. Geometrically, the rotor blades from both experiments are quite similar. In the second experiment, the tip chord length is a little larger, giving a tip chord Reynolds number of 5,500,000, compared to 3,900,000 for the first experiment.

Surface Flow Visualization

Before attempting to interpret the rotor blade surface flow visualization patterns, we first analyzed many photographs together with physical length measurements taken immediately after each test. Figure 2 shows a photograph of the oil-paint pattern on the rotor blade suction surface. The geometric complexities associated with blade lean and twist make such photographs difficult to interpret. Therefore, the resulting patterns have been drawn on projected surfaces. Figure 3 shows the reconstruction of the oil-paint pattern on the suction surface. As discussed further by Zierke, Straka, and Taylor [1993], this figure shows that a rather complex, three-dimensional corner separation exists where the suction surface trailing edge meets the hub. Also, Figure 3 shows that a line of local separation exists on the suction surface, moving from 70% chord near the hub to 96% chord near the tip.

The downstream zone of separation varies from the three-dimensional corner separation near the hub--including the spiral node of separation--to a more two-dimensional type of separation over most of the span. Just upstream of this local separation line, the skin-friction lines begin to migrate radially outward. Also, skin-friction lines emanating from the pressure surface have moved around the trailing edge within the separation zone--similar to the skin-friction lines on the stator blades of Schulz and Gallus [1988]--and also migrate radially outward. The reason for this radial motion in an otherwise two-dimensional flow can be seen from an evaluation of the radial equilibrium equation,

$$\frac{1}{\rho}\frac{\partial p}{\partial r} = \frac{V_\theta^2}{r} + \frac{V_m^2}{R_c} + \frac{1}{\rho}F_r \, .$$

Within the blade passage, the positive centripetal acceleration term establishes a radial pressure gradient, with the largest pressures occurring near the tip. Note that the negative lean of these rotor blades will increase this radial pressure gradient (through the blade force, F_r), especially near the endwalls. Closer to the suction surface (within the boundary layers), the tangential velocities become larger and, at the blade surface, they take on the value of the blade rotational speed. This increase in V_θ creates an imbalance in the radial equilibrium equation, and the larger centripetal acceleration causes fluid to move radially outward.

FIGURE 2. PHOTOGRAPH OF OIL-PAINT PATTERN ON THE ROTOR BLADE SUCTION SURFACE.

Because of the radially outward flow near the trailing edge, the surface of separation that lifts off the blade at the local separation line rolls-up into a spanwise vortex. Near the casing, this vortex moves in the circumferential direction, away from the suction surface as the blade rotates in the other direction. The oil-paint surface flow visualization from the first HIREP experiment showed similar patterns on the suction surface--with a larger corner separation. In addition, we were able to visualize this vortex as it moved away from the suction surface in the circumferential direction by lowering the tunnel pressure until the vortex began to cavitate. Figure 4 shows a typical cavitation photograph of both this vortex and the tip leakage vortex. This

photograph shows that this trailing-edge separation vortex lies closer to the casing than the tip leakage vortex, with both vortices rotating with the same sense. Eventually, the trailing-edge separation vortex rolls-up into the tip leakage vortex as it propagates downstream. In the second HIREP experiment, we were unable to obtain a low enough tunnel pressure for this vortex to cavitate. Evidently, the higher-loaded rotor blades used in the first experiment created a stronger vortex from the trailing-edge separation and the lower pressure within this vortex core led to cavitation at a higher tunnel pressure, as discussed by Farrell and Billet [1994]. However, during a numerical analysis of the second HIREP experiment, Dreyer and Zierke [1993] presented particle paths calculated from their numerical computations that clearly showed the existence of the trailing-edge separation vortex, in addition to the rotor tip leakage vortex.

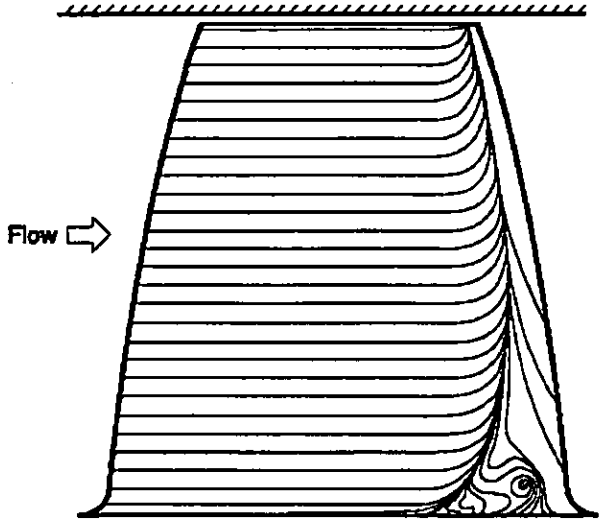

FIGURE 3. SCHEMATIC OF SURFACE FLOW VISUALIZATION ON THE PROJECTED ROTOR BLADE SUCTION SECTION.

The surface flow visualization patterns of Figure 5 show a very two-dimensional flow over the pressure surface. However, one very significant pattern does show up on the pressure surface oil-paint pattern of Figure 5: A radial outward flow exists over the top 8% of the span. This radial flow initiates the flow from the pressure surface through the tip clearance. Figure 6 shows the skin-friction lines associated with the leakage flow across the rotor blade tip section. Notice how these skin-friction lines on the rotor blade tip section are not parallel. Near the leading edge, the skin-friction line was tilted 1 degree from the circumferential direction, while near the trailing edge, the skin-friction line was tilted 16 degrees from the circumferential direction. Also, recall that the pressure side corner of the rotor blade tip section was rounded to prevent local separation of the leakage flow; therefore, the oil-paint pattern shows no sign of separation. From the first HIREP experiment, the oil-paint patterns showed that the angle between the relative skin-friction lines and the chord line decreased with increasing clearance.

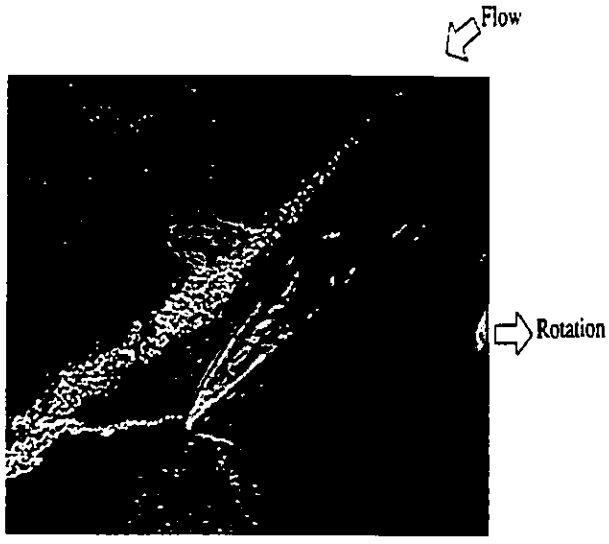

FIGURE 4. PHOTOGRAPH OF A CAVITATING ROTOR TIP LEAKAGE VORTEX AND A CAVITATING TRAILING EDGE SEPARATION VORTEX NEAR A ROTOR BLADE TIP SECTION (FARRELL [1989]).

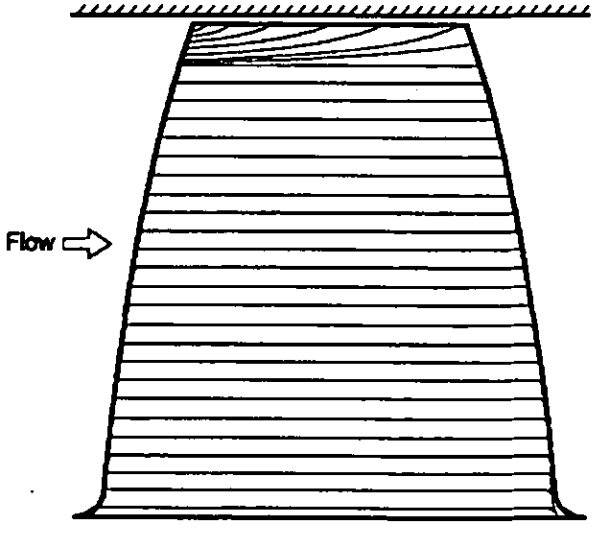

FIGURE 5. SCHEMATIC OF SURFACE FLOW VISUALIZATION ON THE PROJECTED ROTOR BLADE PRESSURE SURFACE.

Visualization of the Rotor Tip Leakage Vortex

The relatively low static pressure within the core of the tip leakage vortex allowed us to visualize cavitation within the core at low tunnel pressures. Photographs and videos showed the existence of some cavitating bubbles originating in the clearance near the rotor blade leading edge. Most of the cavitation,

however, appears to begin near the suction surface at 15% chord--a position very close to the measured minimum pressure point on the suction surface at 90% span, as shown in Figure 7. Inoue and Kuroumaru [1989] and Storer and Cumpsty [1991] contend that the onset of the vortex sheet rolling-up into the tip leakage vortex occurs near the point of minimum pressure on the suction surface. At this location, the pressure difference across the clearance reaches a maximum, creating a larger leakage jet. Therefore, this origin of the vortex marks the position where the core pressure becomes low enough to establish a cavitating flow. For the first HIREP experiment, cavitation visualization showed that the roll-up of the vortex probably originates closer to the leading edge for smaller tip clearances.

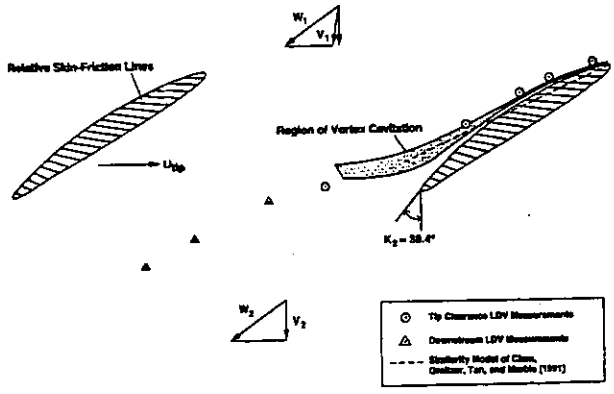

FIGURE 6. SCHEMATIC OF THE RELATIVE SKIN-FRICTION LINES ACROSS THE ROTOR BLADE TIP SECTION AND THE POSITION OF THE ROTOR TIP LEAKAGE VORTEX IN THE BLADE-TO-BLADE PLANE.

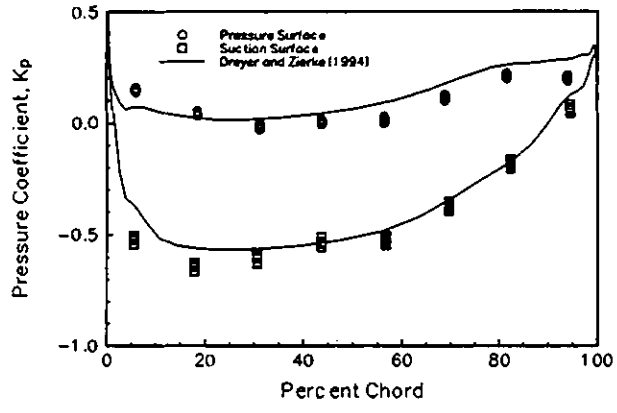

FIGURE 7. ROTOR BLADE STATIC-PRESSURE DISTRIBUTION AT 90% SPAN.

Cavitation visualization showed the circumferential position of the tip leakage vortex within the rotor blade passage. The vortex remains quite close to the suction surface until near 80% chord, where it begins to migrate away from the blade. From the vortex cavitation in the first HIREP experiment, we observed that the circumferential position of the vortex within the passage depended weakly on the tip clearance. For large clearances, the vortex was positioned along the suction surface; for smaller clearances, the vortex was approximately t_{max} away from the suction surface at the trailing edge. After analyzing many photographs--as well as video tapes--from the second experiment, we sketched the envelope that enclosed the cavitating vortices from all seven blades at different times. Figure 6 includes this sketch, along with the relative skin-friction lines across the rotor blade tip section as determined from the surface flow visualization. Downstream of the cavitating part of the tip leakage vortex, Figure 6 shows the circumferential position of the vortex center as determined from the laser Doppler velocimeter (LDV) data at three axial measurement planes--data that will be describe in more detail in the second and companion paper (Zierke, Farrell, and Straka [1994]). Also, we attempted to measure the flow within the clearance region at five chordwise and three radial locations. Within the clearance regions themselves, reflections off the blade tips gave erroneous data. This problem also occurred in the first HIREP experiment for small clearances. However, while the LDV measurement volume was located outside of the clearance regions and within the blade passages, we could measure data. Figure 6 shows our estimates of the circumferential position of the vortex from these LDV measurements. Remember that these estimates are based on data at only three closely spaced radial measurement locations. The uncertainty in the position of the vortex increases near the blade leading edge where the vortex has yet to roll-up and near the trailing edge where the vortex center has moved to a radial position less than that of the LDV measurements.

Before discussing further details of the position of the tip leakage vortex, let us discuss another piece of information included in Figure 6--the position of the vortex core as computed from the model of Chen, Greitzer, Tan, and Marble [1991]. After comparing their complete vortex model with experimental data covering a large range of clearances, loading, and flow coefficients, they found that the vortex trajectories within the blade passage were well described by a single similarity solution curve and equation,

$$\frac{y_c}{x_c} = \frac{0.46\cos(\gamma)}{\phi}\sqrt{\frac{1}{2}(\Delta K_p)_{mean}} \quad ,$$

where y_c is the distance normal to the camber line, x_c is the distance along the blade chord, γ is the stagger angle (58.1 degrees for the HIREP rotor blade tip section), and $(\Delta K_p)_{mean}$ is the difference in K_p across the blade at some mean radius (a radius outside the endwall region). Figure 6 shows the trajectory of the tip leakage flow within HIREP using this similarity solution (y_c = 0.14 x_c). Over the first half of the blade, this zero blade thickness model computes a trajectory that remains within the clearance established by the actual blade thickness. Further downstream, however, the computed trajectory matches very well with the vortex cavitation. Besides the zero blade thickness approximation, another problem may arise when comparing the calculations with measurements near the leading edge. As seen from the pressure distribution at 90% span in Figure 7, the streamwise pressure gradients near the leading edge are larger than

near midchord. Therefore, in the vicinity of the leading edge, the flow acceleration in the streamwise direction may be comparable with the acceleration across the tip clearance and the equations describing these two flow directions should be coupled here--violating the approximations used in the model. Also, recall that the onset of the vortex sheet rolling-up into the tip leakage vortex occurred closer to 15% chord than to the leading edge.

The similarity solution of Chen, Greitzer, Tan, and Marble [1991] holds within the blade passage to a point normal to the camber line at the blade trailing edge. Beyond this point, the trajectory of the tip leakage vortex must be computed using their complete model. The presence and proximity of the casing endwall requires their vortex method of computation to include an image vortex system. Within the blade passage, this image vortex system differs from the one used downstream of the blade passage, and this different image vortex system changes the induced velocities in the tip leakage vortex--giving a slope discontinuity in the vortex core trajectory. They report that even though the actual influence of the blade should drop off in a finite distance, their calculations with this slope discontinuity matched experimental results well. Figure 6 shows that our cavitation visualization also showed a change in slope of the vortex core trajectory at a location normal to the camber line at the blade trailing edge--exactly as the complete model would predict. Further downstream, Figure 6 shows that the trajectory of the vortex core as determined from the LDV measurements has changed slope once again. Here, the vortex core follows the relative flow direction, as determined from a streamline curvature solution, with a 5 degree deviation. Relative to a line tangent to the camber line at the trailing edge, the deviation angle of the vortex core trajectory is 24 degrees. As the vortex loses strength and convects downstream of the rotor blades, one would certainly expect that it would convect with the mean flow.

Another phenomenon occurs in the trailing-edge region that may affect the vortex core trajectory and vortex kinking. As shown in the cavitation photograph in Figure 4 from the first experiment, the trailing-edge separation vortex moves in the circumferential direction, away from the suction surface as the blade rotates in the other direction. Figures 4 also shows that this second vortex lies closer to the casing than the tip leakage vortex. These two vortices pass one another, at different radii, near the trailing-edge plane and the interaction of these two vortices may affect the vortex core trajectory. This interaction should occur for any rotor blades where the centrifugal effects create a radial flow on the suction surface with some trailing-edge separation. In their tip leakage vortex experiment, Inoue and Kuroumaru [1989] also measured a strong radial velocity moving up the suction surface trailing edge into the endwall region. While the trailing-edge separation vortex is smaller in strength than the tip leakage vortex, it can induce an additional downstream velocity component onto the tip leakage vortex which may help the trajectory move back into the relative flow direction. Also, since the two vortices rotate with the same sense, the trailing-edge separation vortex will rotate around the stronger tip leakage vortex if the two vortices are close enough together.

As the tip leakage vortex convects downstream, the position of the vortex core moves radially. Looking through a periscope from a position downstream of the rotor blades, we observed the tip leakage vortex from a video camera during the laser light sheet visualization. The position of each frame in the video corresponded to an individual rotor blade. Visualizing the oncoming vortices at three axial positions of the laser light sheet and analyzing the LDV measurements at three different axial positions allowed us to track the radial position of the tip leakage vortices. Figure 8 presents the radial position of the tip leakage vortex within HIREP. The error bars on the position determined from the laser light sheet visualization represent 95% confidence bands, while the error bars on the positions determined from the LDV data represent the uncertainty that the vortex core may actually lie on an adjacent radial measurement location. Figure 8 shows that most of the radial migration of the vortex core takes place within the blade passage, with only a slight radial migration taking place downstream of the blade trailing edge. The model of Chen, Greitzer, Tan, and Marble [1991] indicates that the vortex core remains at nearly a constant radial location downstream of the trailing edge. Similar to our data, Inoue, Kuroumaru, and Fukuhara [1986] report a small decrease in the radial position of the center of the vortex with streamwise direction.

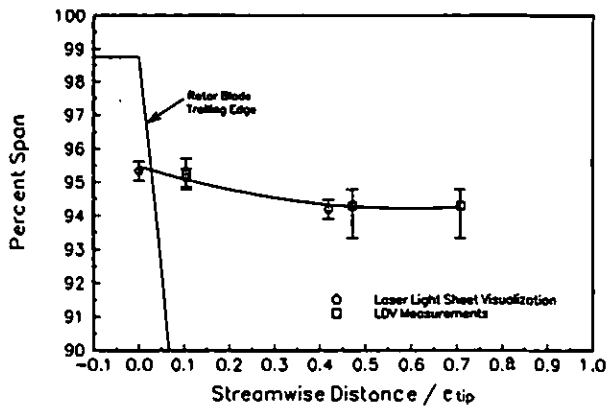

FIGURE 8. SPANWISE POSITION OF THE CORE OF THE ROTOR TIP LEAKAGE VORTEX.

Unsteadiness of the Rotor Tip Leakage Vortex

Aside from giving the location of the tip leakage vortex, both types of flow visualization also showed the unsteadiness of the tip leakage vortex. Other investigators have also observed this spatial vortex wandering. For a tip vortex trailing behind a wing or hydrofoil, Reed [1973] and Baker, Barker, Bohaf, and Saffman [1974] observed oscillations and random wandering of the vortex as it convected downstream and they attributed this unsteadiness to freestream turbulence. Using double-pulsed holography, Green [1988] performed another study of the tip vortex trailing behind a hydrofoil. He found that the primary source of core unsteadiness is associated with global core flow structure instabilities. Reconstruction of holograms allowed him to observe both vortex kinking and a second and rather chaotic unsteadiness that he labelled mini-vortex breakdown. Most of his unsteadiness was located where the initially large axial velocity excess within the vortex core would rapidly decelerate. For flows with a rotor tip clearance, Straka and Farrell [1992] extended the analysis of the tip leakage vortex data acquired in the first HIREP experiment by Farrell [1989] and found the existence of vortex

wandering and kinking. Besides the effects of freestream turbulence and vortex core instabilities, they noted that the unsteady interaction of the rotor blades with the wakes from the inlet guide vanes can contribute to the unsteadiness of the tip leakage vortex. Finally, within an axial-flow turbine, Yamamoto and his colleagues [1993] acquired hot-wire measurements of the tip leakage vortex emanating from the clearance region between stator blades and the endwall located downstream of a row of rotor blades. They found that both the strength and size of the tip leakage vortex changed with time.

Similar to the observations made by Straka and Farrell [1992], we observed unsteady wandering and kinking of the tip leakage vortices in the second HIREP experiment using videos and photographs taken during our cavitation visualization tests. The photograph in Figure 9 shows an example of vortex kinking. While the vortex wandering and kinking appeared at all locations where the vortex core cavitated, this unsteadiness was most evident near the trailing edge where the vortex core trajectory changed slopes. Some interaction with the trailing-edge separation vortex may increase the unsteadiness of the tip leakage vortex. Further downstream, the laser light sheet visualization showed that the tip leakage vortex experienced an unsteady wandering in the circumferential and radial directions. Cavitation visualization from the first HIREP experiment showed that the vortex kinking and oscillating motion were more prevalent for vortices emanating from small tip clearances.

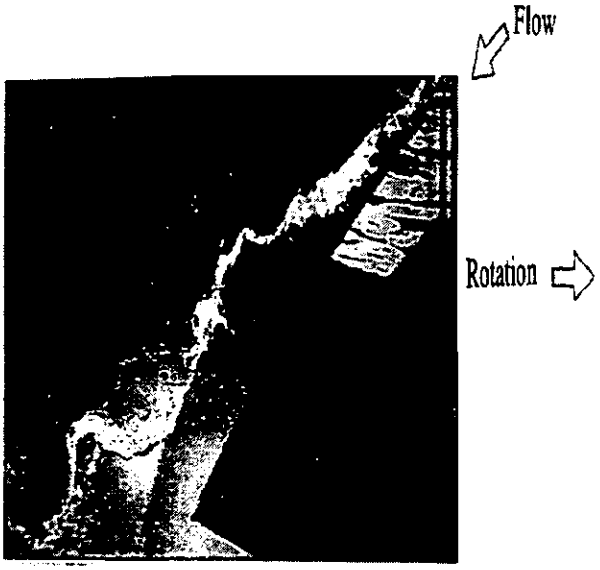

FIGURE 9. PHOTOGRAPH OF A CAVITATING ROTOR TIP LEAKAGE VORTEX WITH VORTEX KINKING.

One detrimental effect of vortex wandering involves time-average flow measurements. Velocity measurements through the vortex core must be fast enough to avoid averaging errors induced by the unsteady motion of the core. For time-average measurements, such as LDV measurements, the effect of vortex wandering is to broaden the measured velocity profiles and reduce the magnitude of the maximum vortex tangential velocity. Straka and Farrell [1992] developed an oscillating vortex model that approximates how vortex wandering affects time-average velocity profiles. Using this model and their data, they applied least-squared cubic curve fits to find empirical relationships between the apparent and instantaneous values of core size and relative maximum tangential velocity. In the second HIREP experiment, we also used cavitation visualization to obtain an amplitude of oscillation in the circumferential direction normalized by an estimate of the vortex core radius, A/r_c = 2.1. For a broadened velocity profile measured with an LDV, the approximate model of Straka and Farrell [1992] uses this parameter to estimate an apparent core radius that is 2.04 times larger than the actual vortex core radius and an apparent maximum relative tangential velocity that is 0.64 times the actual value. In addition, our laser light sheet visualization allowed us to observe the oscillation in the radial direction. While observations allowed us to estimate an amplitude of oscillation in the radial direction of 0.5 cm, we could not estimate the instantaneous core size. Therefore, we could not apply the model of Straka and Farrell [1992] in the radial direction.

SUMMARY

Two experiments have been performed to acquire flow measurements in the rotor blade tip clearance region of a high Reynnlds number pump. The initial experiment involved rotor blades with varying tip clearances, while a second experiment involved a more detailed investigation of a rotor blade row with a single tip clearance. Both experiments included surface flow visualization of the skin-friction line patterns on the rotor blade surfaces and cavitation visualization of the tip leakage vortex. The second experiment also included measurements of the static-pressure distribution at 90% span and some laser light sheet visualization of the tip leakage vortex. While both axial-flow pumps and compressors are subject to many of the same design considerations in regard to tip leakage flows, the use of water flowing through a pump does allow for the use of these unique flow visualization techniques.

The flow visualization on the blade surface and within the flow field indicate that the combination of centripetal acceleration and separation near the trailing edge of the rotor blade suction surface results in the formation of a trailing-edge separation vortex--a vortex which migrates radially upwards along the trailing edge and then tums in the circumferential direction near the casing, moving in the opposite direction of blade rotation. A computational analysis of this rotor corroborates the existence of this secondary vortex. Flow visualization also helps in establishing the trajectnry of the tip leakage vortex core, which exhibits a kink near the trailing edge. The trailing-edge separation vortex, which lies closer to the endwall than the tip leakage vortex, seems to have an influence on this trajectory. Finally, the perindic interaction of the rotor blades with wakes from the upstream inlet guide vanes--as well as freestream turbulence and vortex structure instabilities--will also affect the unsteadiness of the vnrtex. This unsteadiness will lead to averaging errors of time-average flow measurements.

ACKNOWLEDGEMENTS

The first experiment was conducted under the sponsorship of the United States Navy Department, while the second experiment was supported by the Advanced Research Projects Agency.

REFERENCES

Arakawa, C. and Tagori, T., "Fundamental Experiments of Oil Films on a Rotating Disk," *Flow Visualization II*, Edited by W. Merzkirch, pp. 127-131, Proceedings of the Second International Symposium on Flow Visualization, Bochum, West Germany, September 9-12, 1980.

Baker, G. R., Barker, S. J., Bohaf, K. K., and Saffman, P. G., "Laser Anemometer Measurements of Trailing Vortices in Water," *Journal of Fluid Mechanics*, Vol. 65, Part 2, pp. 325-336, 1974.

Betz, A., "The Phenomena at the Tips of Kaplan Turbines," Hydraulische Probleme, 1925.

Chen, G. T., Greitzer, E. M., Tan, C. S., and Marble, F. E., "Similarity Analysis of Compressor Tip Clearance Flow Structure," Transactions of the ASME, *Journal of Turbomachinery*, Vol. 113, pp. 260-271, April 1991.

Dreyer, J. J. and Zierke, W. C., "Solution of the Average-Passage Equations for the Incompressible Flow through Multiple-Blade-Row Turbomachinery," The Pennsylvania State University, Applied Research Laboratory Technical Report, No. TR 94-01, January 1994.

Farrell, K, J., McBride, M. W., and Billet, M. L., "High Reynolds Number Pump Facility for Cavitation Research," ASME International Symposium on Cavitation Research Facilities and Techniques--1987, FED-Vol. 57, edited by J. W. Holl and M. L. Billet, pp. 61-68, 1987.

Farrell, K. J., "An Investigation of End-Wall Vortex Cavitation in a High Reynolds Number Axial-Flow Pump," M.S. Thesis, Department of Mechanical Engineering, The Pennsylvania State University, May 1989.

Farrell, K. J. and Billet, M. L., "A Correlation of Leakage Vortex Cavitation in Axial Flow Pumps," Transactions of the ASME, *Journal of Fluids Engineering*, to appear, 1994.

Gearhart, W. S., "Tip Clearance Cavitation in Shrouded Underwater Propulsors," *AIAA Journal of Aircraft*, Vol. 3, No. 2, March-April 1966.

Green, S. I., "Trailing Vortex Core Unsteadiness--An Exploratory Study of Reynolds Number Effects," AIAA First National Fluid Dynamics Congress, July 1988.

Inoue, M., Kuroumaru, M., and Fukuhara, M., "Behavior of Tip Leakage Flow Behind an Axial Compressor Rotor," Transactions of the ASME, *Journal of Engineering for Gas Turbines and Power*, Vol. 108, pp. 7-14, January 1986.

Inoue, M. and Kuroumaru, M., "Structure of Tip Clearance Flow in an Isolated Axial Compressor Rotor," Transactions of the ASME, *Journal of Turbomachinery*, Vol. 111, pp. 250-256, July 1989.

Lauchle, G. C., Billet, M. L., and Deutsch, S., "High-Reynolds Number Liquid Flow Measurements," *Frontiers in Experimental Fluid Mechanics*, pp. 95-157, edited by M. Gad-el-Hak, Springer-Verlag Berlin Heidelberg, 1989.

Meldahl, A., "The End Losses of Turbine Blades," *The Brown Boveri Review*, Vol. 28, No. 11, pp. 356-361, 1941.

Peacock, R. E., "Blade Tip Gap Effects in Turbomachines, A Review," Naval Posi-Graduate School Report NPS 67-81-016, 1981.

Reed, R. E., "Properties of the Lateral Random Oscillations of Trailing Vortices Observed in Wind-Tunnel Tests," Neilson Engineering and Research, Inc., NEAR TR 47, January 1973.

Reeder, J. A., "Tip Clearance Problems in Axial Compressors (A Survey of Available Literature)," Union Carbide Corporation, Nuclear Division, Report K-1682, 1968.

Schulz, H. D. and Gallus, H. E., "Experimental Investigation of the Three-Dimensional Flow in an Annular Compressor Cascade," Transactions of the ASME, *Journal of Turbomachinery*, Vol. 110, pp. 467-478, October 1988.

Storer, J. A. and Cumpsty, N. A., "Tip Leakage Flow in Axial Compressors," Transactions of the ASME, *Journal of Turbomachinery*, Vol. 113, pp. 252-259, April 1991.

Straka, W. A. and Farrell, K. J., "The Effect of Spatial Wandering on Experimental Laser Velocimeter Measurements of the End-Wall Vortices in an Axial-Flow Pump," *Experiments in Fluids*, Vol. 13, pp. 163-170, 1992.

Yamamoto, A., Mimura, F., Tominaga, J., Tomihisa, S., Outa, E., and Matsuki, M., "Unsteady Three-Dimensional Flow Behavior Due to Rotor-Stator Interaction in an Axial-Flow Turbine," ASME Paper 93-GT-404, Presented at the ASME International Gas Turbine and Aeroengine Congress and Exposition, Cincinnati, Ohio, May 24-27, 1993.

Yaras, M. and Sjolander, S. A., "Review of Studies on Tip Clearance Effects in Axial Turbomachinery," Carleton University, Report No. M&AE 88-3, 1988.

Zierke, W. C., Straka, W. A., and Taylor, P. D., "The High Reynolds Number Flow through an Axial-Flow Pump," The Pennsylvania State University, Applied Research Laboratory Technical Report, No. TR 93-12, November 1993.

Zierke, W. C., Farrell, K. J., and Straka, W. A., "Measurements of the Tip Clearance Flow for a High Reynolds Number Axial-Flow Rotor: Part 2 - Detailed Flow Measurements," presented at the 39th ASME International Gas Turbine and Aeroengine Congress and Exposition, June 13-16, 1994.